Video Article

Correlating Gene-specific DNA Methylation Changes with Expression and Transcriptional Activity of Astrocytic *KCNJ10* (Kir4.1)

Sinifunanya E. Nwaobi[1], Michelle L. Olsen[1]

[1]Department of Cell Developmental and Integrative Biology, University of Alabama at Birmingham

Correspondence to: Michelle L. Olsen at molsen@uab.edu

URL: https://www.jove.com/video/52406
DOI: doi:10.3791/52406

Keywords: Molecular Biology, Issue 103, DNA methylation, MS-HRMA, Luciferase promoter assay, FACS, Astrocytes, Kir4.1, *KCNJ10*

Date Published: 9/26/2015

Citation: Nwaobi, S.E., Olsen, M.L. Correlating Gene-specific DNA Methylation Changes with Expression and Transcriptional Activity of Astrocytic *KCNJ10* (Kir4.1). *J. Vis. Exp.* (103), e52406, doi:10.3791/52406 (2015).

Abstract

DNA methylation serves to regulate gene expression through the covalent attachment of a methyl group onto the C5 position of a cytosine in a cytosine-guanine dinucleotide. While DNA methylation provides long-lasting and stable changes in gene expression, patterns and levels of DNA methylation are also subject to change based on a variety of signals and stimuli. As such, DNA methylation functions as a powerful and dynamic regulator of gene expression. The study of neuroepigenetics has revealed a variety of physiological and pathological states that are associated with both global and gene-specific changes in DNA methylation. Specifically, striking correlations between changes in gene expression and DNA methylation exist in neuropsychiatric and neurodegenerative disorders, during synaptic plasticity, and following CNS injury. However, as the field of neuroepigenetics continues to expand its understanding of the role of DNA methylation in CNS physiology, delineating causal relationships in regards to changes in gene expression and DNA methylation are essential. Moreover, in regards to the larger field of neuroscience, the presence of vast region and cell-specific differences requires techniques that address these variances when studying the transcriptome, proteome, and epigenome. Here we describe FACS sorting of cortical astrocytes that allows for subsequent examination of a both RNA transcription and DNA methylation. Furthermore, we detail a technique to examine DNA methylation, methylation sensitive high resolution melt analysis (MS-HRMA) as well as a luciferase promoter assay. Through the use of these combined techniques one is able to not only explore correlative changes between DNA methylation and gene expression, but also directly assess if changes in the DNA methylation status of a given gene region are sufficient to affect transcriptional activity.

Video Link

The video component of this article can be found at https://www.jove.com/video/52406/

Introduction

Epigenetics is the study of chemical modifications that can affect the transcriptional activity of the genome. Essentially, without a change in the DNA sequence, epigenetic modifications such as DNA methylation, histone acetylation, and histone methylation are sufficient to reversibly alter patterns of gene expression [1]. DNA methylation, a potent regulator of gene expression, is the most well characterized epigenetic modification. DNA methylation is the covalent attachment of methyl groups on the C5 position of a cytosine, typically the cytosine of a cytosine-guanine dinucleotide, also known as a CpG site. Areas that contain a high density of CpG sites are known as CpG islands (CGIs). CGIs are frequently associated with transcriptional start sites (TSS) and gene promoters [1-3]. Thus, while changes in DNA methylation at CGIs are not always concomitant with changes in cellular expression or function, changes in DNA methylation at CGIs can exert powerful regulation on transcriptional activity [2].

Historically, DNA methylation was observed to be essential in embryogenesis, imprinting, and development, with little changes in the levels of DNA methylation occurring in post-mitotic cells (with the exception of alterations in cancer-related genes) [4,5]. However, the field of neuroepigenetics has highlighted an important non-developmental role for DNA methylation. Specifically, cognitive epigenetics has redefined DNA methylation as a highly plastic mechanism integral in mediating both the transcriptional activation and repression of genes essential for the process of learning and memory [6]. Apart from cognitive epigenetics, studies modeling ischemic injury and neuropathic pain characterize DNA methylation as a labile mechanism that responds rapidly to a variety of CNS insults [7-9]. In regards to astrocytes, several lines of evidence suggest DNA methylation plays an important role in astrogliogenesis. Fan *et al.,* found that conditional KO of DNMT1 in neural progenitor cells (NPCs) resulted in precocious development of astrocytes concordant with a global state of hypomethylation [10]. Additionally, Perisic *et al.,* concluded differential levels of DNA methylation of the GLT-1 promoter mediated differential levels of expression of the glutamate transporter in the cortex and cerebellum, emphasizing a role in DNA methylation in establishing brain-region specific patterns of astrocytic gene expression [11]. Overall, numerous studies underscore the dynamic and labile nature of DNA methylation in the CNS as environment, drugs, and injury have all been shown to change DNA methylation and often, gene expression [4,9]. Together, these neuroepigenetic studies point to DNA methylation as a feasible therapeutic target with the potential to mitigate a variety of CNS pathologies.

As the field of epigenetics expands its understanding of the role of DNA methylation in neurodevelopment and disease, the challenge of moving DNA methylation towards a therapeutic target is performing not only correlative, but causative studies that define specific gene targets and sites.

Additionally, surveying changes in DNA methylation specific to brain region and cell type remains an ongoing and time worthy challenge unique to the field of neuroepigenetics. This protocol utilizes a variety of techniques including fluorescence-activated cell sorting (FACS) of astrocytes, methylation-sensitive high resolution melt analysis (MS-HRM), and a methylation luciferase assay to investigate the DNA methylation status of KCNJ10, a gene that encodes for Kir4.1. Kir4.1 is a glial specific potassium channel that demonstrates both brain region and cell specific patterns of expression in the CNS [12-16]. Kir4.1 expression increases moving from rostral to caudal CNS regions, with the highest expression occurring in the spinal cord [15]. Although the channel is expressed in ependymal cells, oligodendrocytes and their precursor cells, Kir4.1 is predominantly expressed in astrocytes and thought to be essential for maintaining homeostatic levels of potassium as well as supporting glutamate uptake by setting the astrocytic resting membrane potential at a hyperpolarized -80mV [12,16-19]. Importantly, the expression of Kir4.1 is non-static both during development and following multiple forms of CNS injury [20-25]. We wished to examine the epigenetic regulation of this channel, specifically in astrocytes during development. The techniques utilized offer gene-specific and targeted CpG site analyses that provide causal evidence for a role of DNA methylation in regulating *KCNJ10* gene expression. These techniques can be applied to other genes.

Protocol

All animals were handled in accordance with the National Institutes of Health guidelines. The Animal Care and Use Committee at the University of Alabama at Birmingham approved animal use.

1. Obtaining RNA and DNA from an Enriched Astrocytic Population using Fluorescent Activated Cell Sorting (FACS) of Astrocytes from Whole Brain Tissue

1. Sedate animal with CO_2 for 1 min and then rapidly decapitate. Dissect cortices as described in Albuquerque *et al.*,[26]; it is not necessary to remove meninges.
   Note: Transgenic rats expressing eGFP under the S100β (an astrocyte marker) promoter were generated by Itakura *et al.*[27] and utilized for FACS sorting of astrocytes.
2. Prepare whole brain homogenate using a papain dissociation kit under non-sterile conditions according to manufacturer's protocol. Heat-activate papain at 37 °C in water bath for 10 min. Note: Papain solution is provided by manufacturer and contains L-cysteine and EDTA (See Table of Materials).
   1. Cut or dremel a hole into the top of a 50 ml conical tube to allow tubing carrying 95%O_2:5% CO_2 to be fed into a closed conical tube (**Figure 1A**). Place dissected cortices in 10mm culture dish containing dissociation media (MEM supplemented with 20mM glucose and penicillin/streptomycin (500 U/ml) and equilibrated to 95%O_2:5% CO_2) and use a clean razor blade to mince tissue into 1 x 1 mm^2 pieces.
3. Transfer tissue using 10 ml manual pipetman to 50 ml conical tube containing papain solution. Allow tissue to settle to bottom of transfer pipette before discharging to minimize the amount of dissociation media carried over. Keep papain solution equilibrated to 95%O_2:5% CO_2 via surface gas exchange for the duration of the incubation. Do not bubble papain solution. Incubate tissue for 20 min in 37 °C water bath.
4. Following incubation in papain solution, triturate tissue 10 times with a 10 ml transfer pipette at slow speed. Centrifuge cloudy cell suspension at 1,000 x g for 5 min at RT.
   1. Equilibrate DNase/albumin inhibitor solution (provided by manufacturer) via surface gas exchange and re-suspend pelleted cells in 3 ml of DNase/albumin inhibitor solution. Prepare commercial discontinuous density gradient following manufacturer instructions.
5. Spin discontinuous density gradient at 1,000 x g for 6 min. Isolate dissociated cells from the bottom of tube by sucking bottom pellet using a pipette.
6. Re-suspend dissociated cells in 2-3 ml of DPBS with 0.02% bovine serum albumin and 1 mg/ml DNase or preferred HEPES buffered culture media. Pass through 40 µm filter before FACS (**Figure 2A**). Keep cells on ice until sorting.
   1. Perform FACS[28].
   2. Pellet cells in 1.5 ml centrifuge tubes at 2,000 x g for 5 min at 4 °C.
      Note: Pelleted astrocytes can be utilized immediately or kept in -80 °C until DNA extraction.
7. Extract RNA and DNA using preferred isolation method [2930]. Assess RNA and DNA concentration and quality via spectrophotometer and bioanalyzer [31].
   Note: Utilize only high quality RNA and DNA in subsequent steps, 260/280=2.0-2.2 and 1.8-1.9, respectively. Bioanalyzer analysis is essential to assess for RNA degradation or DNA fragmentation. RNA or DNA can be utilized immediately or stored in -80 °C or -20 °C, respectively for subsequent studies.

2. Assessing DNA Methylation Status of a Gene using Methylation-sensitive High Resolution Melt Analysis (MS-HRMA)

1. Enter gene sequence of interest into preferred online methylation mapping software to identify any CpG islands in gene of interest [32].
   1. Design primers against bisulfite converted DNA sequence[33] and amplify using preferred DNA polymerase according to manufacturer's protocol. Verify amplified product size by running a 1% agarose DNA gel at 100 V for 45 min. Store primers at stock concentration of 20 µM in -20 °C.
2. Bisulfite convert 500-1,000 ng of DNA of each sample and methylated DNA standards ranging from 0-100% from the same animal species [34]. Elute samples to provide a concentration of 20 ng/µl. Verify concentration of bisulfite converted DNA via spectrophotometer [31].
3. Setup 20 µl reactions for MS-HRM amplification using preferred DNA polymerase and primers at 5 µM concentration according to **Table 1 and 2**. Run all samples, including FACS DNA and methylated standards, in triplicate.

4. Depending on analysis software, set pre- and post- start and stop parameters around the transitions of the melt curve. Set pre-melt start and pre-melt stop parameters so the difference between the two is 0.2 – 0.5 °C. Set post-melt start and post-melt stop similarly. Extract peak temperature difference data for each sample.
5. Using percent methylated standards (y-value) and their corresponding average peak temperature differences (x-value) generate a linear regression equation (**Figure 3A-B**, **Table 3-4**). Use this linear regression equation to estimate methylation status of unknown samples [35].

3. Assessing Hyper-methylated Promoter Activity via Use of Luciferase Assay

1. Identify CpG islands of target gene (Step 2.1). PCR amplify regions of interest [36] and clone upstream of the *luc2* Firefly luciferase reporter gene to produce CpG-island-luc2 plasmids [37].
2. Linearize 30 µg of CpG-island-luc2 plasmid via restriction enzyme digestion [38]. Verify sites for restriction digest and avoid double cuts using preferred cutter software [38]. Heat-inactivate enzymes at appropriate temperature and duration following digestion according to manufacturer's protocol. Minimal loss of DNA occurs during the linearization step.
3. Methylate linearized plasmids using CpG methylase (M.SssI) O/N at 30 °C or leave untreated following manufacturer protocol except for the following adjustments.
4. Perform 50 µl reactions.
5. Use 5 units of CpG methylase to methylate 700 ng of linearized plasmid.
6. Run reactions O/N for 13-19 hr.
7. Following CpG methylase reaction, perform DNA cleanup using standard, commercially available silica-gel membrane clean up kit according to manufacturer's protocol. Significant losses of DNA occur following CpG methylase reaction, 30-60% loss.
8. Verify methylation of plasmids via an Hpa II restriction digest.
9. Take 1 µg of methylated or non-methylated DNA and restriction digest with Hpa II for 1 hr at 37 °C. Use 5-10 units of Hpa II for each µg DNA. Following Hpa II digestion, perform DNA cleanup using preferred, commercially available silica-gel membrane clean up kit. Run both CpG methylated and non-methylated plasmids on a 1% agarose DNA gel in TAE or TBE buffer at 100 V for 45 min for visualization (**Figure 4B**).
10. Subject both methylated and non-methylated plasmids to double digestion with appropriate restriction enzymes to release full-length luc 2 (vector) and CpG island (insert) fragments [38]. Perform double digestion O/N at appropriate temperature and heat-inactivate enzymes following digestion according to manufacturer's protocol. Minimal loss of DNA concentration occurs during double restriction digest.
11. Run double digested plasmids on 1% DNA agarose gel at 100 V for 1 hr to allow for separation of vector and insert (**Figure 4C**). Caution. Wearing protective UV face shield, place DNA gel on a tabletop black light to visualize bands. Based on size, excise methylated and non-methylated insert and non-methylated vector using a clean surgical blade.
12. Gel extract DNA using saturated phenol, pH 6.6. Briefly, weigh DNA gel containing vector or insert. Use 100 µl of phenol per 0.1 gram of DNA gel. Homogenize DNA gel in phenol using glass dounce homogenizer.
13. Add chloroform (using 1/5 of phenol volume) and shake samples for 20 sec. Incubate samples at RT for 2-3 min. Centrifuge for 15 min at max speed (16.1 x 1,000 x g) at 4 °C.
14. Remove aqueous solution and add 0.1X volume of 3 M sodium acetate and 2.5X volume of ethanol. Incubate samples for 1 hr at -80 °C. Following incubation, remove ethanol and re-suspend DNA in 30 µl of preferred buffer. Significant loss of DNA occurs following isolation of inserts and vectors, 30-50% loss.
15. Re-ligate methylated and non-methylated inserts to non-methylated vector using T4 DNA ligase [38]. Use a 1:4 ratio of vector to insert for ligation reactions. Setup reaction according to manufacturer instructions. Use a total volume of 50 µl for reactions and incubate O/N at -20 °C or on ice with lid over ice bucket.
16. Following ligation, perform DNA cleanup using preferred, commercially available silica-gel membrane clean up kit. Significant loss of DNA occur following ligation reaction, an approximate 30-50% loss of DNA. Verify re-ligation by running on 1% agarose DNA gel at 100 V for 45 min and assess concentration of re-ligated plasmids (**Figure 4D**).
17. Transfect methylated or non-methylated plasmids into D54 cells using a commercial transfection reagent according to manufacturer's protocol. Seed D54 cells onto 12-well plate at a 0.14 x 10^6 cells/well.
18. Following 24 hr, transfect cells with equal concentrations of either (1) non-methyated CpG-luc2 plasmid + Renilla or other control luciferase vector or (2) methylated CpG-luc2 plasmid + Renilla or other control luciferase vector.
19. Allow cells to transfect for 24 hr before performing dual luciferase assay. Perform assay according to manufacturer instructions. Perform readings using a luminometer. Read each well in triplicate.
20. Calculate ratio of *Firefly* luciferase activity to *Renilla* or other control luciferase activity. Normalize methylated *Firefly:control* luciferase activity to non-methylated *Firefly:control* luciferase activity by dividing methylated luciferase activity by non-methylated luciferase activity

Representative Results

An enriched population of astrocytes was acquired via FACS sorting of eGFP-S100β transgenic animals [27]. Due to decreasing quality of cells and molecular molecules isolated from animals older than postnatal day 50 (p50), animals aged p0-p40 are optimal for such experiments. Cortical tissue was used for these experiments. Cortices from two to six animals were pooled together. FACS was performed at UAB Comprehensive Flow Cytometry Core facility. Sorting was performed on Becton Dickinson FacsAria II. eGFP excitation was obtained using 488 nm laser; no compensation was necessary. A gated population was targeted based on forward and side scatter (**Figure 1B**). A live cell population was determined using an ethidium bromide dead cell indicator and gated (**Figure 1C**). Two different populations were observed based on the eGFP profile (**Figure 1D**). Through empiric testing, the cell population with higher eGFP profile was identified as the eGFP-positive cell population (**Figure 1F-F"**). Visual analysis of the second population with a lower eGFP profile revealed cell fragments expressing eGFP, but devoid of nuclei, likely representing debris from astrocytic processes (**Figure 1G-G"**). Representative images of dissociated eGFP positive astrocytes following dissociation but prior to sorting (**Figure 2A**) and after sorting (**Figure 2B**) are shown. Isolated eGFP positive cell population demonstrated a 40-fold increase in *ALDH1L1* mRNA, an astrocytic specific marker [39] (**Figure 2C**). Additionally, despite shared expression of S100β in NG2+ OPCs and astrocytes [39], we observed a 4-fold reduction of *NG2* mRNA, a marker for oligodendrocyte precursor cells [39], indicating isolation of an enriched astrocytic cell population (**Figure 2C-D**). RNA and DNA isolated from FACS sorted astrocytes were of sufficient quality and quantity to be used for subsequent methylation studies. Total RNA and DNA isolated from varying ages and number of animals is

listed as a reference for expected yield of molecular molecules following FACS (**Table 5**). It should be noted that the yield will also vary based on number of animals utilized, incubation period, and experience of researcher. **Table 6** demonstrates the variability of events acquired depending on number of animals utilized and incubation periods.

For methylation studies, starting with high quality and sufficient quantities of DNA is essential for successful downstream applications. To ensure sufficient lysis of tissue for RNA or DNA extraction, all homogenization of tissue or cells was followed by trituration using a 23G needle 7x, taking care to avoid frothing during lysis. Once high quality DNA is extracted and bisulfite converted, regions of interest can be targeted for MS-HRMA. Note that when assessing quality and concentration of bisulfite converted DNA, spectrophotometer should be set to read at an OD factor of 33 as bisulfite converted DNA is single stranded. The 260/280 values for bisulfite converted DNA ranged from 2.20-2.70.

Before beginning methylation studies, it is critical to appropriately select and calibrate a thermal cycler for MS-HRMA studies. Additionally, one must determine how to export and utilize raw data generated from MS-HRMA. *Applied Biosystems High Resolution Melting Getting Started Guide* was utilized to assist in calibrating the 7900HT thermal cycler. Finally, data was extracted and imported into HRM analysis software for subsequent data analysis. As detailed in the protocol, pre and post start and stop parameters were set near the transitions of the melt curve. Peak temperature differences were used to extrapolate methylation status of unknown samples. Estimated methylation data acquired from MS-HRMA corresponded closely to methylation data generated from pyrosequencing (pyrosequencing data was generated in house using primers targeting same regions as MS-HRM primers) **(Figure 3C)** [15].

A dual luciferase assay was utilized to assess the transcriptional activity of hyper-methylated regions of the gene of interest (**Figure 4A**). Each CpG-island-luc2 plasmid was linearized and then methylated. However, because both the insert (CpG island) and vector (luc2) are methylated during the reaction, one must excise the methylated insert and re-ligate to a non-methylated vector. Due to extensive manipulation of the plasmid, significant losses occur and one must begin with sufficient starting material. HpaII digestion was utilized to verify the methylation status of each plasmid as HpaII only digests non-methylated DNA (**Figure 4B**). It should be noted that if O/N methylation is insufficient, an additional 1x of SAM and 1x of CpG methylase may be added following 1 hr of incubation at 30 °C. Continue O/N incubation following addition of supplemental SAM and CpG methylase. Generation of methylated and non-methylated CpG-island-luc2 plasmid allows for direct assessment of changes between DNA methylation and transcriptional activity via measurement of luciferase activity.

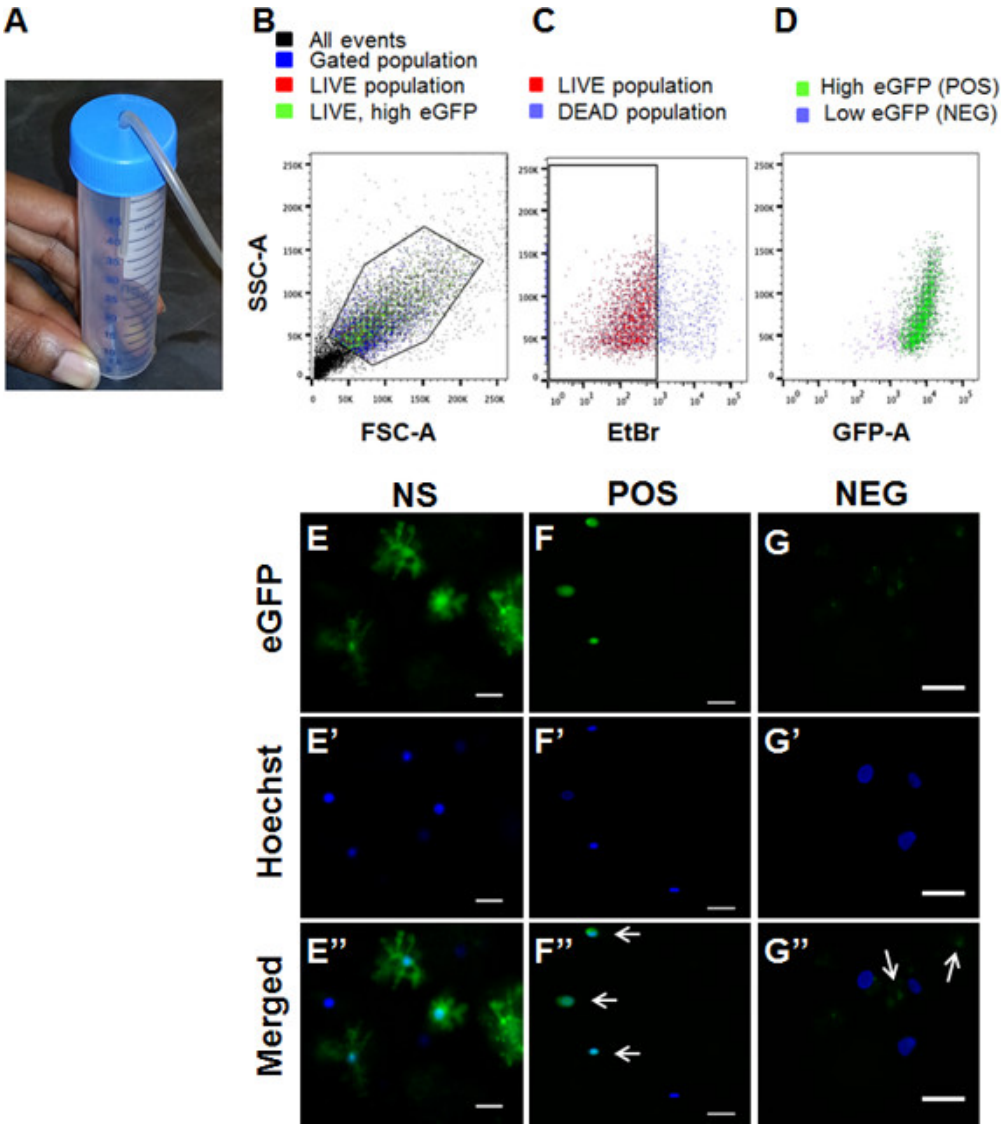

Figure 1. FACS sorting isolates eGFP+ cell popoulation. (**A**) Use of a 50 ml conical tube with hole cut on the top allows for surface gas exchange during papain digestion. (**B**) Sorted cells were gated based on forward and side scatter plots. (**C**) An ethidium bromide based dead cell indicator was utilized to gate a live cell population (red). (**D**) Live cell population demonstrated two populations - one with a high eGFP profile (green) and a low eGFP profile (purple). For all graphs, y-axis represents side scatter area (SSC-A); x-axis represents forward side scatter area (FSC-A), green fluorescent protein area (GFP-A), or ethidium bromide (EtBr). (**E-G**) Dissociated cells were incubated with Hoechst and 20 µl of dissociated cells was placed on coverslip and imaged. (**E-E"**) eGFP+ astrocytes, with extensive processes were visualized before sorting (NS). (**F-F"**) Following sorting, high eGFP+ population (POS) demonstrate eGFP+ cell soma which co-localize with Hoechst staining. (**G-G"**) Low eGFP population demonstrates eGFP+ staining which did not co-localize with Hoechst staining, likely representing astrocytic debris (for all images, scale = 20 µm). Please click here to view a larger version of this figure.

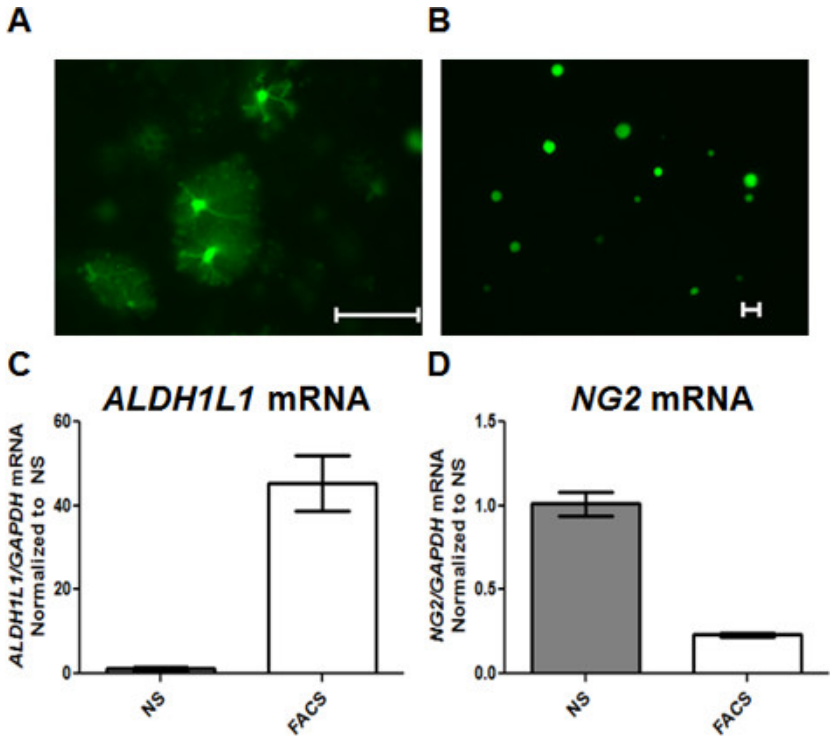

Figure 2. FACS sorting of eGFP-S100β transgenic animals provides enriched population of astrocytes. (**A**) 20 µl of dissociated cells before FACS (NS) are shown, processes remain intact (scale =50 µm). (**B**) Representative image post-FACS (FACS) cells are shown; astrocytic processes are removed and cell soma remains (scale =20 µm). (**C**) qPCR data demonstrates a 40-fold increase in *ALDH1L1* mRNA in FACS sorted cells (FACS) compared to not sorted population (NS). (**D**) *NG2* mRNA is reduced by 4-fold in FACS sorted cells compared to not sorted population (NS). Please click here to view a larger version of this figure.

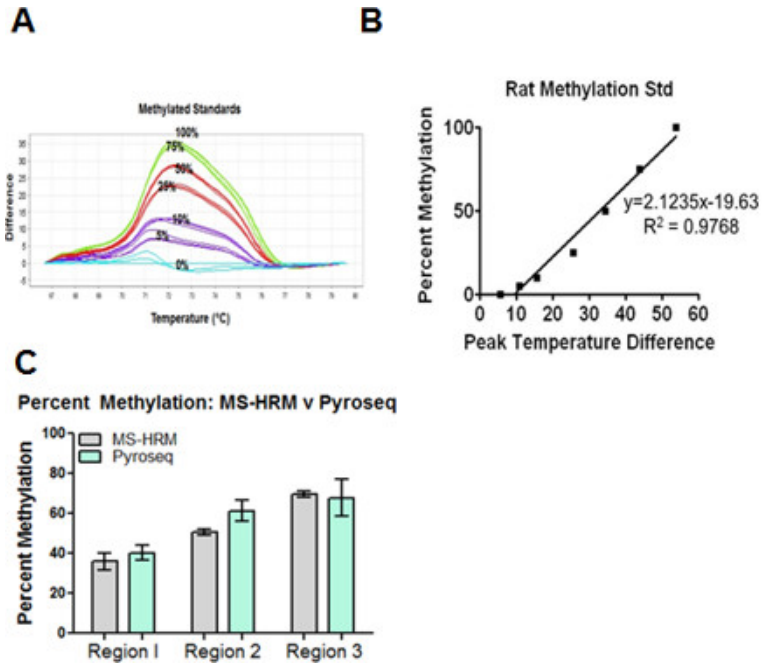

Figure 3. Sample data and analysis for MS-HRM studies. (**A**) Example of temperature difference plots generated from methylation standards. Corresponding percent methylation is labelled for each curve (**B**) Example of linear regression equation generated from rat methylated standards. (**C**) Comparison of the percent methylation acquired from pyrosequencing (pyroseq, green bars) and MS-HRMA (gray bars) demonstrates similar levels of methylation for varying regions of *KCNJ10*. Pyrosequencing data generated in house using primers targeting same regions as MS-HRM analysis. Please click here to view a larger version of this figure.

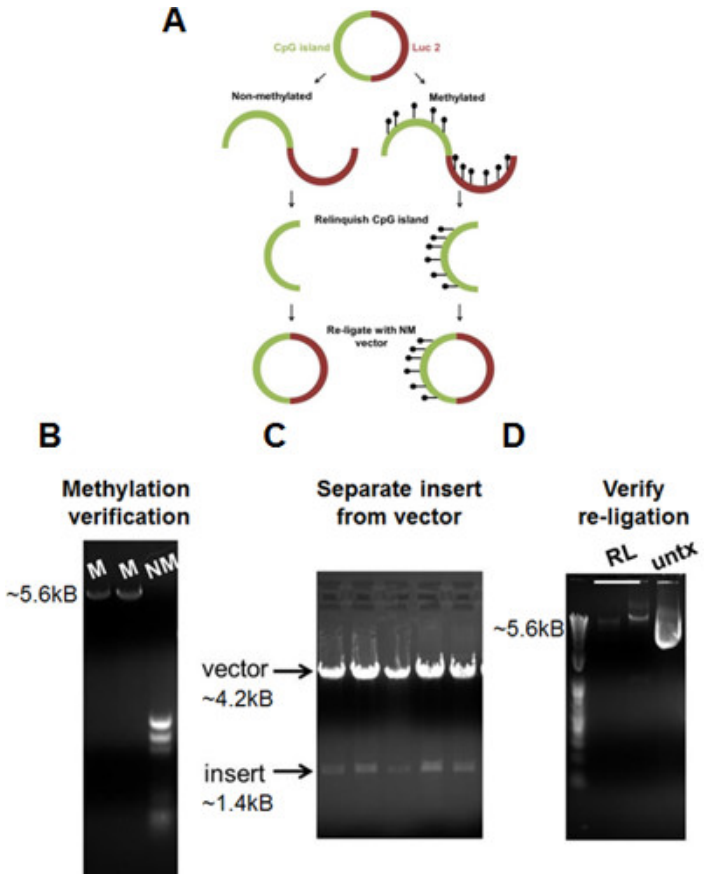

Figure 4. Dual luciferase assay allows for assessment of transcriptional activity of differentially methylated gene regions. (**A**) **Diagram of luciferase transcriptional activity assay demonstrates workflow of protocol. (B**) DNA gel displays differences in methylated versus non-methylated plasmids following HpaII digestion. Non-methylated DNA is readily digested following HpaII digestion compared to methylated DNA, demonstrating successful methylation of DNA plasmid. (**C**) DNA gel demonstrates separation of vector from insert following double digestion. Following DNA separation, vector and insert are gel extracted. (**D**) DNA gel demonstrates successful re-ligation of vector and insert. Re-ligated plasmid possesses similar molecular weight as untreated plasmid (untx). NM, non-methylated; M, methylated; RL, re-ligated; untx, untreated. Please click here to view a larger version of this figure.

.	Volume (µl)	x3 + 10% excess	x # of samples
MeltDoc MM	10 µl	33 µl	
Primer 1	1.2 µl	3.96 µl	
Primer 2	1.2 µl	3.96 µl	
gDNA	1 µl	---	
dH_20	6.6 µl	21.78 µl	

Table 1. Sample calculation of MeltDoctor Mastermix. Run each MS-HRM reaction in triplicate with 10% excess to compensate for pipetting error. Last column indicates calculation needed for multiple numbers of samples. Total volume for each reaction is 20 µl.

Cycle	Temp (°C)	Time (sec)	Ramp rate (%)
	95 °C	:15	100
40x	95 °C	:15	100
	60 °C	:60	100
Melting parameters	95 °C	:10	100
	60 °C	:60	100
	95 °C	:15	1
	60 °C	:15	100
Hold	4 °C		

Table 2: Sample protocol for amplification. Denature samples at 95 °C for 10 min followed by 40 cycles of amplification and generation of melt curve. Melting parameters are listed within table. Note change in ramp rate that allows for acquisition of high- resolution melting temperature.

Percent Methylation (Rat Standard)	Peak Temperature Difference
y	x
0	5.670116
5	10.70448
10	15.5044
25	25.52295
50	34.43047
75	43.80894
100	53.88717

Table 3. Example of peak temperature difference data. Percent methylation standard is labelled as y-coordinate. Peak temperature difference data is labelled as x-coordinate. Representative peak temperature difference data was acquired using MS-HRM from one gene region.

Peak Temp Difference	Estimated methylation
X	Y
Sample 1 (n=4)	
47.450	81.115
46.292	78.657
41.694	68.894
47.292	80.779
Sample 2 (n=4)	
29.925	43.904
24.269	31.894
25.061	33.575
25.389	34.272

Table 4. Example of calculated estimated percent methylation. Peak temperature difference of samples of unknown methylation status is used to estimate percent methylation using a linear regression equation. Representative data from two different conditions, Sample 1 and Sample 2, are shown; n=4 for each condition.

Age	Number of animals	Total RNA (ng)	Total DNA (ng)
p4-p10	3-6	455-868	265-1523
p19-p22	1-2	220-680	583-1483
p40-p50	3-4	198-260	578-1700

Table 5. Total RNA and DNA acquired from FACS sorted cells. Age and number of animals used in FACS experiments are listed. Note, both cortices were utilized for each N. Total RNA and DNA is listed as a reference for expected yield.

Age	Number of animals	Pos Events	Neg Events	Incubation time (at 37 °C)
p26	1	2.18X10^6	1.15X10^6	20:00 min
p26	2	4.4X10^6	2.78X10^6	20:00 min
p26	2	9.2X10^6	3.3X10^6	30:00 min

Table 6. Number of events acquired from FACS at postnatal day 26. At p26 number of positive (eGFP+) events and negative events varies depending on number of animals utilized and incubation period.

Discussion

This protocol describes the isolation of an enriched population of astrocytes via FACS as well as a variety of techniques that allow for both correlative and causative studies between DNA methylation and gene expression. These techniques, used in isolation or in combination, are particularly useful for laboratories that work with tissue of high cellular heterogeneity or are interested in the DNA methylation status of a particular gene or gene region versus global DNA methylation changes. One relatively unique challenge in studying the epigenome of the CNS is

the diversity of cell populations. As genes of interest may be expressed to varying degrees with both temporally and spatially unique patterns in the CNS, the use of whole tissue often confounds data from both transcription and DNA methylation studies.

Kir4.1, the protein of interest, is spatially and temporally regulated in astrocytes, oligodendrocytes, and ependymal cells [13,14,40-47]. Thus, the use of eGFP-S100β transgenic animals [27] for FACS provided an enriched population of astrocytes [15], and therefore a more accurate assessment of the level of gene transcription and DNA methylation specific to this cell population. Despite this advantage, the use of FACS sorted astrocytes presents several challenges. Preparation of a cell suspension for FACS requires significant disruption of whole tissue and several changes in the temperature and external media environment. While pH and temperature are maintained to promote cell viability and stabilize cellular machinery, it is reasonable to assume that some changes in DNA methylation occur subsequent to the mechanical and enzymatic disruption of cells. Additionally, in comparison to the use of whole tissue, FACS sorting of astrocytes yields significantly lower amounts of RNA and DNA for downstream molecular studies. This low ratio of yield to labor/reagent may limit the feasibility of some studies depending on the number and complexity of subsequent molecular applications as well as brain regions under study. Taking time to maintain proper pH and temperature as well as working efficiently to reduce total protocol time will aid in isolating healthy cells and thus high quality DNA/RNA.

In regards to methylation studies, a variety of applications are currently available for detection of DNA methylation [48,49]. Methylation sensitive high resolution melt analysis (MS-HRMA) was utilized to study *KCNJ10*, the gene of interest. MS-HRMA is useful in screening changes in DNA methylation of any given region of a gene of interest. This technique incorporates many of the same basic concepts and procedures as standard PCR amplification [50]. Thus, reactions can be setup using a number of thermal cyclers and data analysis performed in most laboratories familiar with standard molecular techniques. One caveat to MS-HRMA is that the method provides estimates of the methylation status of a given region of DNA. This is in contrast to pyrosequencing which provides exact percentages of methylation of specific CpG sites. Additionally, depending on the number of CpG sites assessed within one region, using a linear regression may skew results for those regions with limited numbers of CpG sites.

In studying the ability of DNA methylation to regulate *KCNJ10* gene expression, we supplemented correlative studies with a dual luciferase assay to directly assess changes in the transcriptional activity of the *KCNJ10* gene following hypermethylation. Use of the luciferase assay allows for alteration of the methylation status of a specific region of the gene and subsequent assessment of transcriptional activity directly related to these changes. Two major challenges of the luciferase assay are the laborious nature of the protocol and the loss of DNA input through each sequential step. Validation of the quantity and quality of DNA following each reaction as well as starting with a sufficient amount of DNA is essential to acquiring adequate amounts of DNA for transfection. Overall, the use of these techniques can be performed using tools found in most molecular laboratories and be can performed without the use of a large genomic sequencing facility, making these techniques widely accessible to investigators interested in DNA methylation.

Disclosures

The authors have no disclosures.

Acknowledgements

This work was supported by R01NS075062-01A1. FACS sorting performed at UAB Comprehensive Flow Cytometry Core facility (P30 AR048311, P30 A1027767). Dr. Scott Philips from the UAB Neurobiology Core facility and Dr. Susan Nozell from UAB CDIB assisted with technical aspects of the luciferase assay.

References

1. Bird, A. DNA methylation patterns and epigenetic memory. *Genes Dev.* **16** (1), 6-21, doi:10.1101/gad.947102 (2002).
2. Deaton, A.M., & Bird, A. CpG islands and the regulation of transcription. *Genes Dev.* **25** (10), 1010-1022, doi:25/10/1010 [pii];10.1101/gad.2037511 (2011).
3. Lorincz, M.C., Dickerson, D.R., Schmitt, M.,, & Groudine, M. Intragenic DNA methylation alters chromatin structure and elongation efficiency in mammalian cells. *Nat Struct. Mol Biol.* **11** (11), 1068-1075, doi:nsmb840 [pii];10.1038/nsmb840 (2004).
4. Moore, L.D., Le, T.,, & Fan, G. DNA methylation and its basic function. *Neuropsychopharmacol.* **38** (1), 23-38, doi:npp2012112 [pii];10.1038/npp.2012.112 (2013).
5. Santos, K.F., Mazzola, T.N.,, & Carvalho, H.F. The prima donna of epigenetics: the regulation of gene expression by DNA methylation. *Braz.J.Med.Biol.Res.* **38** (10), 1531-1541, doi:S0100-879X2005001000010 [pii];/S0100-879X2005001000010 (2005).
6. Day, J.J., & Sweatt, J.D. Cognitive neuroepigenetics: a role for epigenetic mechanisms in learning and memory. *Neurobiol. Learn.Mem.* **96** (1), 2-12, doi:S1074-7427(10)00228-5 [pii];10.1016/j.nlm.2010.12.008 (2011).
7. Denk, F., & McMahon, S.B. Chronic pain: emerging evidence for the involvement of epigenetics. *Neuron.* **73** (3), 435-444, doi:S0896-6273(12)00094-3 [pii];10.1016/j.neuron.2012.01.012 (2012).
8. Endres, M. *et al.* DNA methyltransferase contributes to delayed ischemic brain injury. *J. Neuroscience.* **20** (9), 3175-3181, (2000).
9. Qureshi, I.A., & Mehler, M.F. Emerging role of epigenetics in stroke: part 1: DNA methylation and chromatin modifications. *Arch.Neurol.* **67** (11), 1316-1322, doi:67/11/1316 [pii];10.1001/archneurol.2010.275 (2010).
10. Tian, R. *et al.* Alexander disease mutant glial fibrillary acidic protein compromises glutamate transport in astrocytes. *J Neuropathol. Exp Neurol.* **69** (4), 335-345, doi:10.1097/NEN.0b013e3181d3cb52;00005072-201004000-00002 [pii] (2010).
11. Perisic, T., Holsboer, F., Rein, T.,, & Zschocke, J. The CpG island shore of the GLT-1 gene acts as a methylation-sensitive enhancer. *Glia.* **60** (9), 1345-1355, doi:10.1002/glia.22353 (2012).
12. Olsen, M.L., Higashimori, H., Campbell, S.L., Hablitz, J.J.,, & Sontheimer, H. Functional expression of Kir4.1 channels in spinal cord astrocytes. *Glia.* **53** (5), 516-528, doi:10.1002/glia.20312 (2006).

13. Poopalasundaram, S. *et al.* Glial heterogeneity in expression of the inwardly rectifying K+ channel, Kir4.1, in adult rat CNS. *Glia.* **30** (4), 362-372, doi:10.1002/(SICI)1098-1136(200006)30:4<362::AID-GLIA50>3.0.CO;2-4 (2000).
14. Hibino, H., Fujita, A., Iwai, K., Yamada, M.,, & Kurachi, Y. Differential assembly of inwardly rectifying K+ channel subunits, Kir4.1 and Kir5.1, in brain astrocytes. *J.Biol.Chem.* **279** (42), 44065-44073, doi:10.1074/jbc.M405985200;M405985200 [pii] (2004).
15. Nwaobi, S.E., Lin, E., Peramsetty, S.R.,, & Olsen, M.L. DNA methylation functions as a critical regulator of Kir4.1 expression during CNS development. *Glia.* **62** (3), 411-427, doi:10.1002/glia.22613 (2014).
16. Li, L., Head, V.,, & Timpe, L.C. Identification of an inward rectifier potassium channel gene expressed in mouse cortical astrocytes. *Glia.* **33** (1), 57-71, doi:10.1002/1098-1136(20010101)33:1<57::AID-GLIA1006>3.0.CO;2-0 [pii] (2001).
17. Kucheryavykh, Y.V. *et al.* Downregulation of Kir4.1 inward rectifying potassium channel subunits by RNAi impairs potassium transfer and glutamate uptake by cultured cortical astrocytes. *Glia.* **55** (3), 274-281, doi:10.1002/glia.20455 (2007).
18. Djukic, B., Casper, K.B., Philpot, B.D., Chin, L.S.,, & McCarthy, K.D. Conditional knock-out of Kir4.1 leads to glial membrane depolarization, inhibition of potassium and glutamate uptake, and enhanced short-term synaptic potentiation. *J. Neuroscience.* **27** (42), 11354-11365, doi:27/42/11354 [pii];10.1523/JNEUROSCI.0723-07.2007 (2007).
19. Fujita, A. *et al.* Clustering of Kir4.1 at specialized compartments of the lateral membrane in ependymal cells of rat brain. *Cell Tissue Res.* **359** (2), 627-634, doi:10.1007/s00441-014-2030-6 (2015).
20. MacFarlane, S.N., & Sontheimer, H. Electrophysiological changes that accompany reactive gliosis *in vitro*. *J Neuroscience.* **17** (19), 7316-7329, (1997).
21. Ambrosio, R., Maris, D.O., Grady, M.S., Winn, H.R.,, & Janigro, D. Impaired K(+) homeostasis and altered electrophysiological properties of post-traumatic hippocampal glia. *J. Neuroscience.* **19** (18), 8152-8162, (1999).
22. Anderova, M. *et al.* Voltage-dependent potassium currents in hypertrophied rat astrocytes after a cortical stab wound. *Glia.* **48** (4), 311-326, doi:10.1002/glia.20076 (2004).
23. Olsen, M.L., Campbell, S.C., McFerrin, M.B., Floyd, C.L.,, & Sontheimer, H. Spinal cord injury causes a wide-spread, persistent loss of Kir4.1 and glutamate transporter 1: benefit of 17 beta-oestradiol treatment. *Brain.* **133** (Pt 4), 1013-1025, doi:awq049 [pii];10.1093/brain/awq049 (2010).
24. Koller, H., Schroeter, M., Jander, S., Stoll, G.,, & Siebler, M. Time course of inwardly rectifying K(+) current reduction in glial cells surrounding ischemic brain lesions. *Brain Res.* **872** (1-2), 194-198, doi:S0006-8993(00)02434-3 [pii] (2000).
25. Bordey, A., Lyons, S.A., Hablitz, J.J.,, & Sontheimer, H. Electrophysiological characteristics of reactive astrocytes in experimental cortical dysplasia. *J Neurophysiol.* **85** (4), 1719-1731, (2001).
26. Albuquerque, C., Joseph, D.J., Choudhury, P.,, & MacDermott, A.B. Dissection, plating, and maintenance of cortical astrocyte cultures. *Cold Spring Harb.Protoc.* **2009** (8), db, doi:2009/8/pdb.prot5273 [pii];10.1101/pdb.prot5273 (2009).
27. Itakura, E. *et al.* Generation of transgenic rats expressing green fluorescent protein in S-100beta-producing pituitary folliculo-stellate cells and brain astrocytes. *Endocrinology.* **148** (4), 1518-1523, doi:en.2006-1390 [pii];10.1210/en.2006-1390 (2007).
28. Foo, L.C. Purification of astrocytes from transgenic rodents by fluorescence-activated cell sorting. *Cold Spring Harb.Protoc.* **2013** (6), 551-560, doi:2013/6/pdb.prot074229 [pii];10.1101/pdb.prot074229 (2013).
29. Smith, C., Otto, P., Bitner, R.,, & Shiels, G. A silica membrane-based method for the isolation of genomic DNA from tissues and cultured cells. *CSH. Protoc.* **2006** (1), doi:2006/1/pdb.prot4097 [pii];10.1101/pdb.prot4097 (2006).
30. Sambrook, J., & Russell, D.W. A Single-step Method for the Simultaneous Preparation of DNA, RNA, and Protein from Cells and Tissues. *CSH. Protoc.* **2006** (1), doi:2006/1/pdb.prot4056 [pii];10.1101/pdb.prot4056 (2006).
31. Barbas, C.F., III, Burton, D.R., Scott, J.K.,, & Silverman, G.J. Quantitation of DNA and RNA. *CSH. Protoc.* **2007** db, (2007).
32. Zhao, Z., & Han, L. CpG islands: algorithms and applications in methylation studies. *Biochem. Biophys. Res. Commun.* **382** (4), 643-645, doi:S0006-291X(09)00541-5 [pii];10.1016/j.bbrc.2009.03.076 (2009).
33. Srivastava, G.P., Guo, J., Shi, H.,, & Xu, D. PRIMEGENS-v2: genome-wide primer design for analyzing DNA methylation patterns of CpG islands. *Bioinformatics.* **24** (17), 1837-1842, doi:btn320 [pii];10.1093/bioinformatics/btn320 (2008).
34. Patterson, K., Molloy, L., Qu, W.,, & Clark, S. DNA methylation: bisulphite modification and analysis. *J.Vis.Exp.*(56), doi:3170 [pii];10.3791/3170 (2011).
35. Drummond, G.B., & Vowler, S.L. Categorized or continuous? Strength of an association-and linear regression. *Adv.Physiol Educ.* **36** (2), 89-92, doi:36/2/89 [pii];10.1152/advan.00046.2012 (2012).
36. Sambrook, J., & Russell, D.W. The basic polymerase chain reaction. *CSH.Protoc.* **2006** (1), doi:2006/1/pdb.prot3824 [pii];10.1101/pdb.prot3824 (2006).
37. Arpa, P. Strategies for cloning PCR products. *Cold Spring Harb.Protoc.* **2009** (8), db, doi:2009/8/pdb.ip68 [pii];10.1101/pdb.ip68 (2009).
38. Makovets, S. Basic DNA electrophoresis in molecular cloning: a comprehensive guide for beginners. *Methods Mol.Biol.* **1054** 11-43, doi:10.1007/978-1-62703-565-1_2 (2013).
39. Cahoy, J.D. *et al.* A transcriptome database for astrocytes, neurons, and oligodendrocytes: a new resource for understanding brain development and function. *J Neuroscience.* **28** (1), 264-278, doi:28/1/264 [pii];10.1523/JNEUROSCI.4178-07.2008 (2008).
40. Maldonado, P.P., Velez-Fort, M., Levavasseur, F.,, & Angulo, M.C. Oligodendrocyte precursor cells are accurate sensors of local K+ in mature gray matter. *J Neuroscience.* **33** (6), 2432-2442, doi:33/6/2432 [pii];10.1523/JNEUROSCI.1961-12.2013 (2013).
41. Kalsi, A.S., Greenwood, K., Wilkin, G.,, & Butt, A.M. Kir4.1 expression by astrocytes and oligodendrocytes in CNS white matter: a developmental study in the rat optic nerve. *J.Anat.* **204** (6), 475-485, doi:10.1111/j.0021-8782.2004.00288.x;JOA288 [pii] (2004).
42. Higashi, K. *et al.* An inwardly rectifying K(+) channel, Kir4.1, expressed in astrocytes surrounds synapses and blood vessels in brain. *Am.J.Physiol Cell Physiol.* **281** (3), C922-C931, (2001).
43. Olsen, M.L., Higashimori, H., Campbell, S.L., Hablitz, J.J.,, & Sontheimer, H. Functional expression of Kir4.1 channels in spinal cord astrocytes. *Glia.* **53** (5), 516-528, doi:10.1002/glia.20312 (2006).
44. Neusch, C., Rozengurt, N., Jacobs, R.E., Lester, H.A.,, & Kofuji, P. Kir4.1 Potassium Channel Subunit Is Crucial for Oligodendrocyte Development and *In Vivo* Myelination. *J. Neuroscience.* **21** (15), 5429-5438, (2001).
45. Kofuji, P. *et al.* Genetic Inactivation of an Inwardly Rectifying Potassium Channel (Kir4.1 Subunit) in Mice: Phenotypic Impact in Retina. *J. Neuroscience.* **20** (15), 5733-5740, (2000).
46. Kofuji, P., & Connors, N.C. Molecular substrates of potassium spatial buffering in glial cells. *Mol.Neurobiol.* **28** (2), 195-208, doi:MN:28:2:195 [pii];10.1385/MN:28:2:195 (2003).
47. Nwaobi, S.E., Lin, E., Peramsetty, S.R.,, & Olsen, M.L. DNA methylation functions as a critical regulator of Kir4.1 expression during CNS development. *Glia.* **62** (3), 411-427, doi:10.1002/glia.22613 [doi] (2014).

48. Wojdacz, T.K., Dobrovic, A.,, & Hansen, L.L. Methylation-sensitive high-resolution melting. *Nat.Protoc.* **3** (12), 1903-1908, doi:nprot.2008.191 [pii];10.1038/nprot.2008.191 (2008).
49. Wojdacz, T.K., & Dobrovic, A. Methylation-sensitive high resolution melting (MS-HRM): a new approach for sensitive and high-throughput assessment of methylation. *Nucleic Acids Res.* **35** (6), e41, doi:gkm013 [pii];10.1093/nar/gkm013 (2007).
50. Laird, P.W. Principles and challenges of genomewide DNA methylation analysis. *Nat.Rev.Genet.* **11** (3), 191-203, doi:nrg2732 [pii];10.1038/nrg2732 (2010).

